J. Fluid Mech. (1971), *vol.* 50, *part* 3, *pp.* 545–563
Printed in Great Britain

A non-linear investigation of critical levels for internal atmospheric gravity waves

By R. J. BREEDING

Department of Earth and Planetary Sciences, Massachusetts Institute of Technology and Advanced Study Program, National Center for Atmospheric Research

(Received 5 June 1970 and in revised form 7 April 1971)

The behaviour of internal gravity waves near a critical level is investigated by means of a transient two dimensional finite difference model. All the important non-linear, viscosity and thermal conduction terms are included, but the rotational terms are omitted and the perturbations are assumed to be incompressible. For Richardson numbers greater than 2·0 the interaction of the incident wave and the mean flow is largely as predicted by the linear theory – very little of the incident wave penetrates through the critical level and almost all of the wave's energy and momentum are absorbed by changes in the original wind. However, these changes in the wind are centred above the critical level, so that the change in the wind has only a small effect on the height of the critical level. For Richardson numbers less than 2·0 and greater than 0·25 a significant fraction of the incident wave is reflected, part of which could have been predicted by the linear theory. For these stable Richardson numbers a steady state is apparently reached where the maximum wind change continues to grow slowly, but the minimum Richardson number and wave magnitudes remain constant. This condition represents a balance between the diffusion outward of the added momentum and the rate at which it is absorbed. For Richardson numbers less than 0·25, over-reflexion, predicted from the linear theory, is observed, but because the system is dynamically unstable no over-reflecting steady state is ever reached.

1. Introduction

The height at which the horizontal component of the phase velocity of an internal gravity wave is equal to the wind speed (both being measured relative to the ground) is called a singular level or a critical level. At this height the irrotational, inviscid adiabatic, linearized equations are singular and the Doppler or intrinsic frequency is zero. This simple set of equations, at this height, is then an inadequate approximation to the real physical world. This inadequacy is confirmed by the fact that this set of equations predicts infinite values for the perturbation wave density and horizontal motion at a critical level.

The implications of the irrotational, inviscid, adiabatic, linearized equations for internal gravity wave behaviour near a critical level have been explored by Bretherton (1966), Booker & Bretherton (1967) and Jones (1968). These analyses have been extended by Jones (1967) to include the Coriolis force but this inclusion does not remove the singularity. The singularity may be removed by

the inclusion of the thermal conduction and viscous terms, or by the inclusion of the non-linear terms. Hazel's (1967) linear analysis of the set of equations in which the viscosity and conduction terms were included showed that the Reynolds stress or the vertical flux of horizontal momentum of a wave incident on a critical level was attenuated almost exactly by the factor

$$f = \exp\left[2\pi(Ri_c - 0{\cdot}25)^{\frac{1}{2}}\right]$$

given by Booker & Bretherton (1967). Ri_c is the Richardson number at the critical level.

In the present report the above results are extended by the inclusion in the set of equations of all the important non-linear terms. The Coriolis terms, however, could not be included. This set of equations is analytically intractable, so the investigation is carried out by means of a finite-difference model. An unperturbed atmosphere containing a shear layer is set up and then a wave for which this shear layer contains a critical level is allowed to propagate into the shear layer and interact with the mean flow there. For computational reasons the wave perturbations were assumed to be incompressible. This is not a serious restriction since it can be shown that the compressible equations approach ever closer to the incompressible equations as a critical level is approached.

2. The mathematical basis of the model

The equations on which this model is based are in the streamfunction vorticity form:

$$\frac{\partial \xi}{\partial t} = -\frac{\partial}{\partial x}[U\xi + g\rho] - \bar{\rho}\frac{\partial}{\partial z}\left(\frac{w\xi}{\bar{\rho}}\right) + \mu\nabla^2\left(\frac{\xi}{\bar{\rho}}\right) + \bar{\rho}w\frac{d^2\bar{u}}{\partial z^2}, \tag{1a}$$

$$\frac{\partial \rho}{\partial t} = -\frac{\partial}{\partial x}\left[U\rho - \frac{\omega_B^2\psi}{g}\right] - \frac{1}{\bar{\rho}}\frac{\partial}{\partial z}(\bar{\rho}w\rho) + K\nabla^2\rho, \tag{1b}$$

$$\nabla^2\psi = \xi, \tag{1c}$$

$$\bar{\rho}u = -\partial\psi/\partial z, \quad \bar{\rho}w = \partial\psi/\partial x, \tag{1d}$$

where x = east–west position, positive eastward, z = vertical position, positive upward, $w = w(x,z,t)$ = vertical perturbation motion, $u = u(x,z,t)$ = horizontal perturbation motion, $\bar{u} = \bar{u}(z)$ = initial horizontal motion (original wind), $U = \bar{u} + u$ = total horizontal motion, K = coefficient of thermometric conductivity, μ = coefficient of dynamic viscosity, ξ = vorticity, $\rho = \rho(x,z,t)$ = perturbation density, $\bar{\rho} = \bar{\rho}(z)$ = ambient density and g is the acceleration due to gravity. Note that ψ and ξ are formed from momentum variables rather than from the more commonly used velocity variables and that $\bar{u}$ is a function of z only, and it is usually taken to be a piecewise linear function so that $d^2\bar{u}/dz^2$ may be ignored.

By using momentum variables throughout, equations (1) can be derived in a straightforward manner from Newton's law and the conservation equations:

$$\bar{\rho}\left[\frac{Du}{Dt} + w\frac{d\bar{u}}{dz}\right] = -\frac{\partial p}{\partial x} + \mu\nabla^2 u, \tag{2a}$$

$$\bar{\rho}\frac{Dw}{Dt} = -\frac{\partial p}{\partial z} - g\rho + \mu\nabla^2 u, \tag{2b}$$

$$\frac{\partial}{\partial x}(\bar{\rho}u) + \frac{\partial}{\partial z}(\bar{\rho}w) = 0, \tag{2c}$$

$$\frac{D\rho}{Dt} + \bar{\rho}w\left(\frac{\omega_B^2}{g}\right) = K\nabla^2\rho, \tag{2d}$$

where $$\omega_B = \left[\frac{2}{\bar{\rho}}\left(\frac{d\bar{\rho}}{dz} - \frac{1}{c^2}\frac{d\bar{\rho}}{dz}\right)\right]^{\frac{1}{2}} = \text{Brunt–Väisälä frequency},$$

$p = p(x, z, t)$ = perturbation pressure and $\bar{p} = \bar{p}(z)$ = ambient pressure. The background pressure and density have been removed from equation (2*b*) by means of the hydrostatic equation. Equation (2*c*) is used instead of the more common $\nabla . \mathbf{v} = 0$, where $\mathbf{v} = \mathbf{a}_x u + \mathbf{a}_z w$ = perturbation velocity, because the additional term $w(d\bar{\rho}/dz)$ was about one-tenth the size of the other two terms in the linear and weakly non-linear regions. (The exact relative size will of course depend on the vertical wavelength.) Thus the background atmosphere remains compressible while the perturbations are incompressible. In the adiabatic equation (2*d*) the speed of sound has been allowed to approach infinity thereby eliminating the pressure terms and acoustic waves. This allows the use of much larger time steps than those which could be used if the acoustic waves were included. Because linear theory predicts that the perturbation pressure p becomes increasingly small as a critical level is approached the absence or presence of these pressure terms should not markedly affect the interactions near a critical level.

Although the initial wind $\bar{u}$ is not allowed to change in time this in no way restricts the non-linear interactions. The total wind is $U = \bar{u} + u$ and a change in the wind appears as that portion of u which is independent of x. The stream function and the vorticity are considerably simplified by this division of the total horizontal motion. Those non-linear terms which depend on the size of the perturbation density with respect to the background density have not been included here. A thorough analysis showed that they were not important at low altitudes.

The Coriolis terms have not been included in Newton's law because three-dimensional models are not feasible at this time. According to Jones (1967) the addition of only the Coriolis terms to the linear, inviscid, irrotational equations does not remove the singularity, and does not much alter the basic wave behaviour from that predicted without the Coriolis force.

It should be noted that if all the lengths and velocities in (1) or (2), and g are multiplied by some factor F and μ, K, and ψ are multiplied by F^2, then the magnitudes of all the equations are unchanged. Consequently the results of this model are largely independent of the wavelengths used. Because of the use of (1), the waves inherent in this model do not possess the $\exp(z/2H)$ growth which characterizes internal gravity waves when the compressibility is included or when the regular incompressible system of equations is used and the Boussinesq approximation is not made. Since this is an investigation of interactions which occur in a height range that is a fraction of a scale height this lack of exponential

growth is no drawback. In the derivation of the vorticity equation the z dependence of the ambient density $\bar{\rho}$ has not been ignored anywhere and all the terms involving $d\bar{\rho}/dz$ have been retained, so it is not strictly correct to say that the Boussinesq approximation has been made. Nevertheless, in some important respects the resulting equations are equivalent to the regular incompressible system of equations when the Boussinesq approximation has been made.

3. The finite-difference model

The finite-difference model was originally closely based on that of Foldvik & Wurtele (1967) but in the course of its development many changes have been made. The grid system is staggered as shown in table 1. In an 'expanded region' around the critical level the value of Δz is smaller than that used elsewhere in the model. This reduction is necessary in order to have the source and the critical

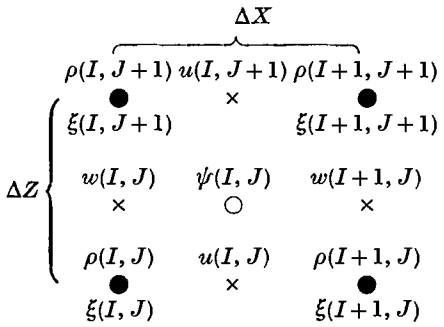

TABLE 1. Staggered grid system. I = integer denoting x position, J = integer denoting z position

level separated by more than half the vertical wavelength and still have sufficient resolution near the critical level. (The use of the fine vertical spacing throughout the model would waste much computer time. If the source and the shear zone are not separated by one half the vertical wavelength or more the shear zone is not initially free of perturbations.)

All the non-linear critical level interactions took place in the expanded region; the region with large Δz was used only to allow an incoming wave to be set up and to allow propagation away from the interaction region. The results reported here were obtained using a model with $\Delta z = 200$ m outside the expanded region and $\Delta z = 25$ m inside the expanded region. The effect of varying Δz both inside and outside the expanded region was explored, and figure 1 compares the magnitude of the fundamental and the constant components of the horizontal motion at $t = 4350$ sec for three different vertical spacings. While differences are evident, they are not considered to be significant.

Large discontinuities in the wave variables caused by the abrupt change of Δz at the boundary of the expanded region were found to occur only when there were large non-linear interactions occurring at that height. By making the expanded region large enough to more than include all of the height range in

which non-linear interactions were taking place between the wave and the mean flow these problems were avoided. The exact extent of the expanded region did not affect the results. For example, with a shear region extending from 2000 to 2800 m, a case with the region from 1800 to 3600 m expanded was compared with a case with the region from 2000 to 3200 m expanded, and differences were found to be a few per cent at most. This agreement also indicates that reflexion from the boundary of the expanded region is not significant.

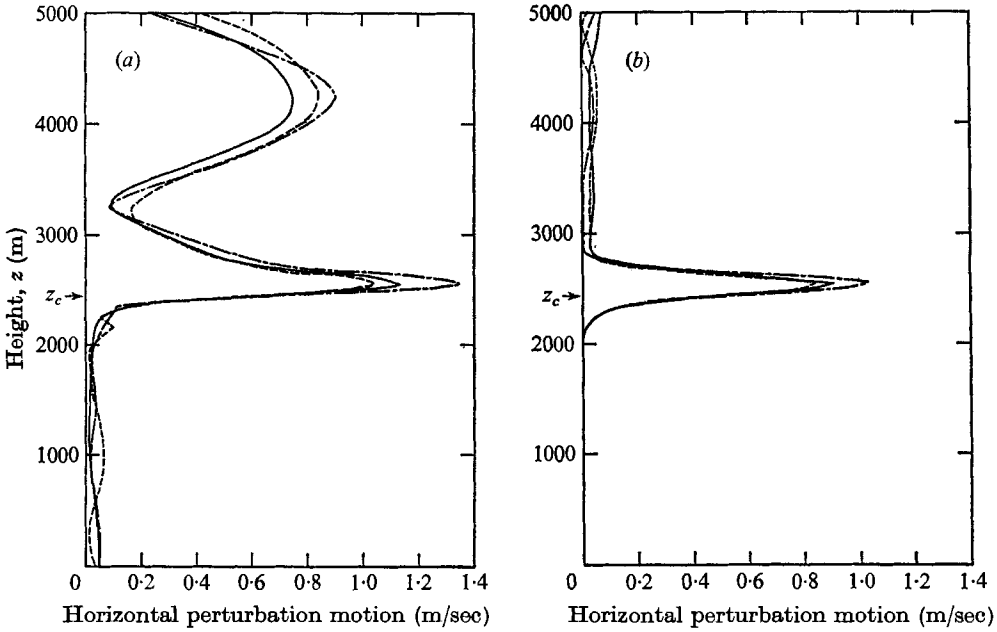

FIGURE 1. Dependence of the fundamental, (*a*), and constant, (*b*), on the vertical spacing. t = 4350 sec; S_s = 1·125 m/sec; Ri = 0·53; ——, Δz = 200, 25; — · —, Δz = 100, 25; – – –, Δz = 100, 12·5.

Since the second and higher harmonics are propagating only for a narrow range of wind speeds near the centre of the shear layer, disturbances with short vertical extent which would be greatly affected by the change in Δz become evanescent at heights near those at which they were generated and so are quite small at the boundary of the expanded region. It was not possible to try the model with a uniform Δz = 25 m throughout to assess all the effects that might be due to the presence of the expanded region because the size of the computer memory did not permit placing the source far enough from the shear layer. However, a case was run with a uniform Δz of 100 m and, although this spacing was too coarse to model the region around the critical level accurately, the results were in qualitative agreement with the other cases.

The effects of varying the values of Δx have also been investigated. The model has been run with eight, sixteen and thirty-two points per horizontal wavelength. (The fundamental wavelength λ_x or the wavelength of the source is meant unless otherwise specified.) The rate of non-linear interactions increases with the number

of points per horizontal wavelength. With only eight points per wavelength the model is obviously of marginal accuracy. Since Δt must be reduced when Δx is reduced, the computation time is proportional to the square of the number of points per wavelength and the thirty-two points per wavelength case took so long to run that only two runs of moderate length were deemed justifiable. Comparison of the sixteen and thirty-two point cases showed that the basic nature of the development of the critical level interactions did not differ although the rates of the non-linear interactions varied by about 10 % between the two models. The finite-difference model was tested for insensitivity to the direction of wave propagation by running two cases which were identical except that the wave and wind were moving to the right in one case and to the left in the other. The results were identical to three significant figures.

The partial derivatives in equations (1 *a*), (1 *b*) and (1 *d*) are transformed into centred finite differences in a straightforward manner. For example, with $x = I\Delta x$, $z = J\Delta z$ and $t = L\Delta t$, the first three terms in equation (1 *a*) are treated as follows:

$$\partial\xi/\partial t \to [\xi(I,J,L+1)-\xi(I,J,L-1)]/2\Delta t,$$

$$\partial(\bar{u}\xi)/\partial x \to \bar{u}[\xi(I+1,J,L)-\xi(I-1,J,L)]/2\Delta x,$$

$$\partial(\bar{u}\xi)/\partial x \to u(I,J,L)\times\tfrac{1}{2}[\xi(I+1,J,L)+\xi(I,J,L)]/\Delta x - u(I-1,J,L) \times \tfrac{1}{2}[\xi(I,J,L)+\xi(I-1,J,L)]/\Delta x.$$

The only exception to the centring of the finite differences in time and space is that the damping terms $\mu\nabla^2(\xi/\bar{\rho})$ and $K\nabla^2\rho$ are evaluated at $t = (L-1)\Delta t$ for stability reasons.

After $\xi(I,J,L+1)$ has been found for all I, J from the finite-difference form of (1 *a*) the stream function ψ is found from (1 *c*) and then, to complete the advance of one time step, the momentum variables are found from (1 *d*). Early in this project Poisson's equation was solved for ψ by relaxation as Foldvik & Wurtele (1967) had done. When the smaller value of Δz around the critical level was introduced, however, the relaxation failed to converge. T. R. Madden (personal communication) suggested that Poisson's equation be solved by means of Fourier analysis and synthesis. In this method each row of vorticity points is treated as a source function in an otherwise source-free region and the analytically determined solutions for each row are then summed. The number of points in the horizontal, however, is required to be an integer power of two so that the fastest Fourier transform methods can be used.

A moving top boundary was an unsatisfactory source because the perturbations are incompressible in this system and the motions so introduced filled the model at once. A line vorticity source does not present such problems. At each step, then, before Poisson's equation is solved, the values of ξ in the chosen row are replaced by

$$\xi_s \cos(kx-\omega t) = \xi_s \cos[2\pi(x/\lambda_x)-(t/\tau)],$$

where k is the horizontal wavenumber, ω is the wave frequency (radians) relative to the ground and τ is the wave period. Because it is $\xi\Delta z$ which actually enters

the solution of Poisson's equation, so that the source strength S_s is independent of the vertical spacing, $\xi_s = S_s/\Delta z$ is used where S_s is independent of the spacing. S_s has the units of velocity and is roughly twice the magnitude of perturbation velocities developed in the case of propagation into an infinite medium. Since the experimental records obtained at Massachusetts Institute of Technology have been associated with waves propagating down to the ground from the jet stream (Madden & Claerbout 1968), the source has been placed at the top of the model and the wave which it generates travels down through a region of constant wind into the shear zone.

Boundaries in the horizontal have been avoided by using cyclical boundary conditions. The repetition or cyclical length of the model is λ_x, the wavelength of the source. In the vertical, a rigid surface upon which $w = 0$ or $\psi =$ constant is the natural lower boundary. The upper vertical boundary presents more problems. A rigid boundary causes reflexions and a free surface upon which $p =$ constant is difficult to incorporate into the model because the pressure has been eliminated from the equations. A steady-state outgoing-wave condition imposed at the top boundary gave poor results with the transient waves in the early stages of this model. The best results have been obtained by reflecting the top portion of the model around the source. In the solution of Poisson's equation ψ is the summation of the contributions from each row of ξ points. To reflect the top portion of the model about the source, the contributions from non-existent rows of ξ above the source are included in this summation and the first row above the source is taken to have the same values of ξ as the first row below the source, the second row above the source to have the same values as the second row below the source and so on. Because the importance of the contribution from a row of ξ values decreases as its distance from the height at which ψ is to be evaluated increases and because ψ is never evaluated above the source, the inclusion of ten or twenty rows of ξ above the source in the summation for ψ is sufficient. This treatment, suggested by T. R. Madden (personal communication), allows the waves to propagate upward just as they do downward. Effects due to waves entering the model from the top boundary have not been noticed.

The centred time step or leap-frog method has been used throughout this work. The occasional forward time step used by Foldvik & Wurtele (1967) was slightly detrimental in this project. The Adams–Bashforth method (Lilly 1965) was also tried but it was no more accurate or stable than the leap-frog method. The stability limit for the linearized finite-difference scheme was determined by the methods of Richtmyer (1957). The model was tested for accuracy by eliminating the wind and the non-linear and damping terms, placing a rigid boundary on the top of the model and initially inserting a standing wave into the model. The model at any later time can then be compared with the linear solutions. When the time step Δt was chosen to minimize the error, the average normalized error grew to 14 % after twenty wave periods. Whether the value of Δt was chosen to minimize the error or not, the error was mainly due to a phase shift, the error in wave magnitude remaining less than a few per cent.

The eddy values initially used for the dynamic viscosity μ and the thermometric conductivity K were too small to eliminate the non-linear aliasing errors

which occurred after the wave motion in the smaller wavelengths had reached a sizeable fraction of the wave motion in the fundamental. The damping coefficients, therefore, were adjusted upward until these aliasing errors disappeared. No change in the interactions near the critical level were noticed when the damping terms were changed by an order of magnitude.

4. Results

A thorough discussion of the results of this finite-difference model requires a brief review of the predictions which can be made from the linearized equations. The gravity wave, propagating downward in a region where $\bar{u} > v_{px} = \omega/k$, will have negative vertical components of the phase and group velocities. The Reynolds stress, taken here to be the product $\bar{\rho}uw$ averaged over λ_x, and the vertical energy flux density will be positive indicating a downward transfer of

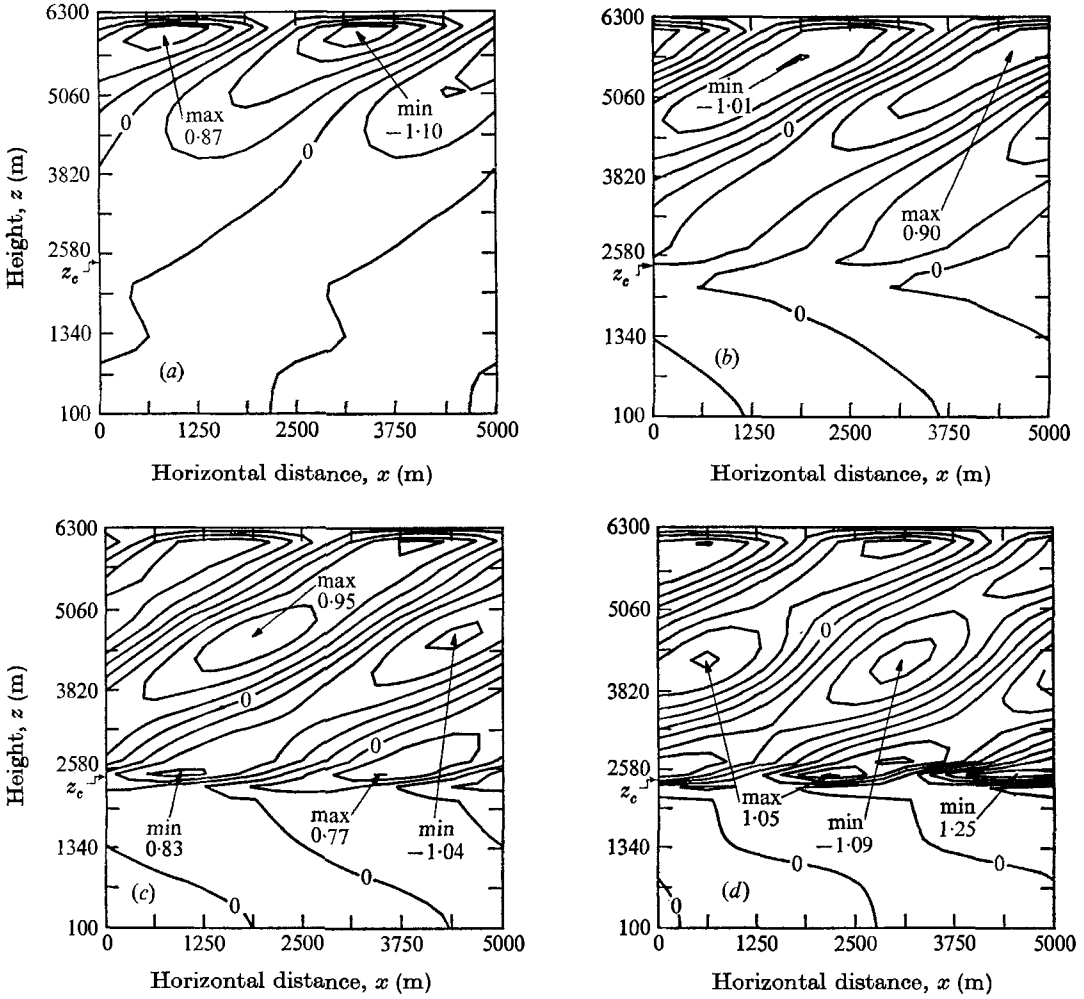

FIGURE 2*a–d*. For legend see facing page.

negative horizontal momentum and negative energy density. Absorption of all or part of the wave will therefore decrease the wind near the critical level. The Reynolds stress and kinetic energy of the wave are expected to be attenuated by the factor f mentioned in the introduction. In applying this factor to the kinetic energy (but not to the Reynolds stress) the energies must be compared at heights on either side of the critical level where $|\bar{u}-v_{px}|$ is the same. In detail, the linearized equation predicts that $\lambda_z \propto \Omega$; u and $\rho \propto 1/\Omega^{\frac{1}{2}}$, and w and $p \propto \Omega^{\frac{1}{2}}$, where Ω = Doppler or intrinsic frequency, relative to the local fluid $= k(v_{px}-\bar{u}) \to 0$ as a critical level is approached and λ_z = vertical wavelength. This increase in u and decrease in λ_z are responsible for the importance of the non-linear terms and the eventual inapplicability of all analyses based on the linearized equations.

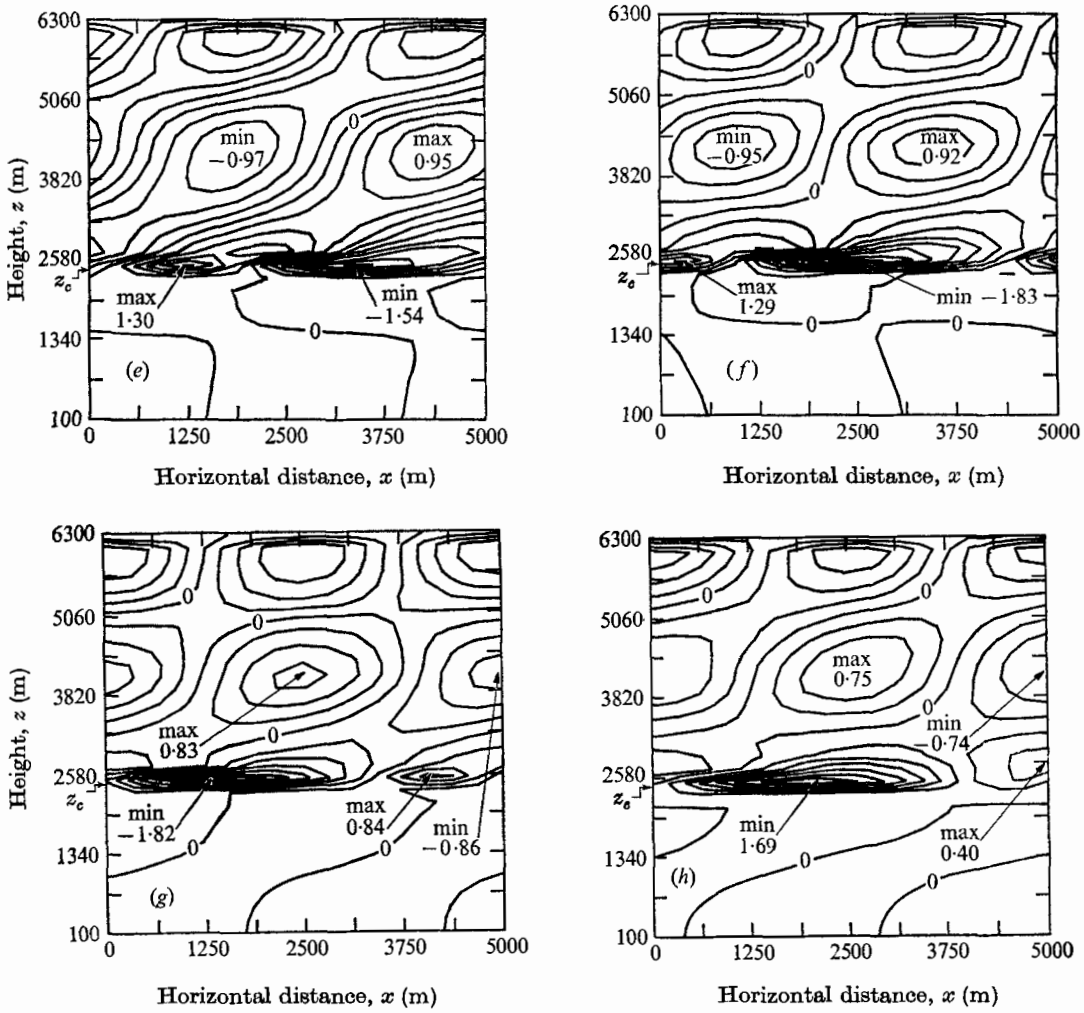

FIGURE 2. Contour plots of u, the horizontal component of the perturbation velocity. S_s = 1·125 m/sec, Ri = 0·53, (*a*) t = 390 sec, (*b*) t = 750 sec, (*c*) t = 1100 sec, (*d*) t = 1470 sec, (*e*) t = 1830 sec, (*f*) t = 2190 sec, (*g*) y = 2550 sec, (*h*) t = 4350 sec.

The internal gravity waves recorded on the microbarograph array in eastern Massachusetts have been associated with propagation downward to the ground from jet-stream heights (Madden & Claerbout 1968) and this has been reflected in setting up this model in that the wind in the lower portion of the model is zero and the source is located at the top of the model in a region of non-zero wind (measured relative to the ground). The orientation has no bearing on the wave–wind interaction and no effects attributable to the presence of a rigid surface beyond the critical level (as seen from the source) have been observed, so the

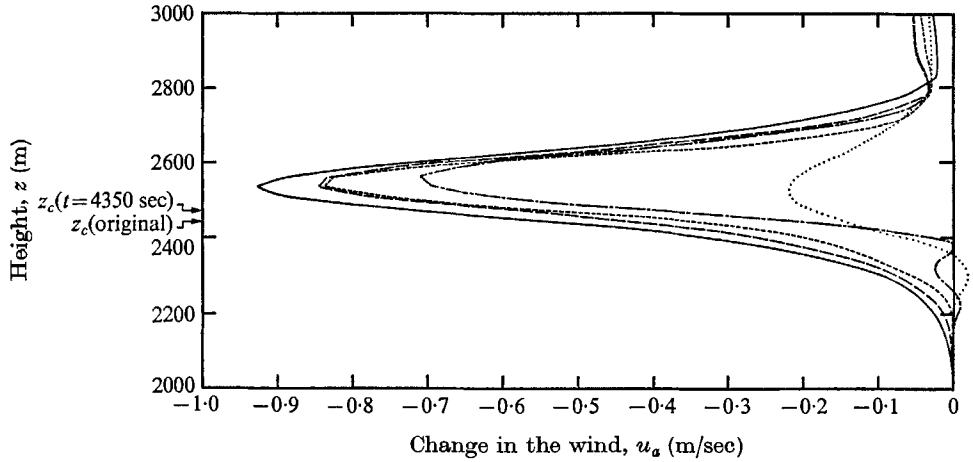

FIGURE 3. Development of the change in the wind with time. $S_s = 1{\cdot}125$ m/sec; $Ri = 0{\cdot}53$; ....., $t = 1470$ sec; —·—, $t = 2190$ sec; - - - - -, $t = 2710$ sec; — —, $t = 3630$ sec; —, $t = 4350$ sec.

results of this model may be applied to any wave–wind critical level interaction which is not close to some boundary. A wave with $\lambda_x = 5000$ m, $\tau = 450$ sec, $v_{px} = 11{\cdot}11$ m/sec is within the range of values commonly recorded by this microbaragraph array so these values have been used throughout except where indicated otherwise.

For all the results presented here, a line vorticity source at $z = 6300$ m was used and the wind varied from zero at the ground to 20 m/sec at the top of the model. Except in one case (discussed below) the wind speed was a linear function of height, being constant above and below the shear layer and having a constant first derivative (or shear) within that layer. The bottom of this shear zone was maintained at 2000 m and different Richardson numbers and shears were obtained by varying the height of the top of the shear zone. Placing the top of the shear zone at 2400 m, 2800 m and 3600 m gave Richardson numbers of 0·133, 0·531 and 2·12 respectively. A constant Brunt–Väisälä period of 345 sec was used. The background density was that of an isothermal atmosphere, $\bar{\rho} = 1{\cdot}225 \exp(z/H)$ kg/m^3 with $H = 8440$ m.

The development of the reference case, Richardson number = $Ri = 0{\cdot}53$, $S_s = 1{\cdot}125$ m/sec is shown in figure 2 by means of a sequence of contour plots of u, the horizontal component of the perturbation fluid velocity (z_c indicates the height of the critical level). The propagation of the wave downward from the

source and its interaction with the shear layer are evident. Note that by 1830 sec the wave pattern above the shear zone is very similar to that of a standing wave and that after 2550 sec there is little change in the basic pattern. The change in the wind continues to increase, however, as shown in figure 3. The values of the wind, Richardson number and the Fourier components of u at

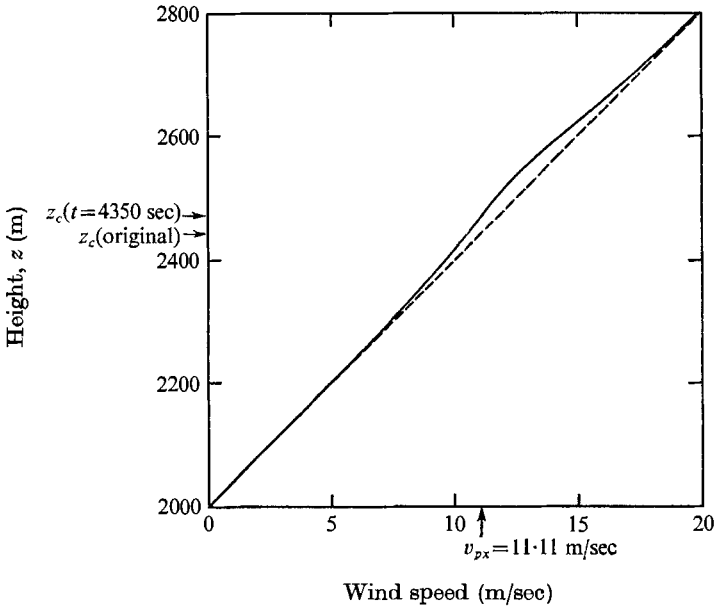

FIGURE 4. Wind S_s = 1·125 m/sec; Ri = 0·53; – – –, original wind; ——, total wind at t = 4350 sec.

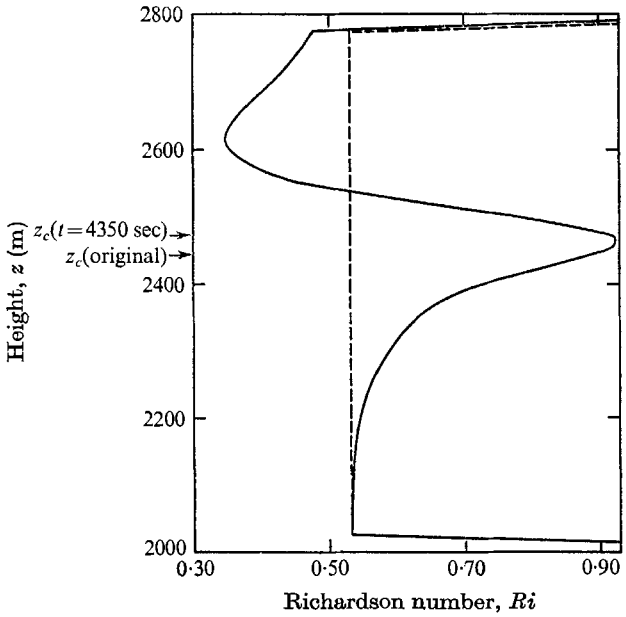

FIGURE 5. Richardson number. S_s = 1·125 m/sec; – – –, original; ——, t = 4350 sec.

t = 4350 sec, after almost ten wave periods, are shown in figures 4–7. It is obvious that the interaction of the wave and the wind occurs above the critical level and that only a small fraction of the wave motion gets through the shear zone. Note that the Richardson number has increased at the critical level. By 4350 sec the critical level has moved up to 2472 m from its original location at 2444 m. (It is assumed that the wave is moving with the horizontal phase speed of the source in determining the position of the critical level.)

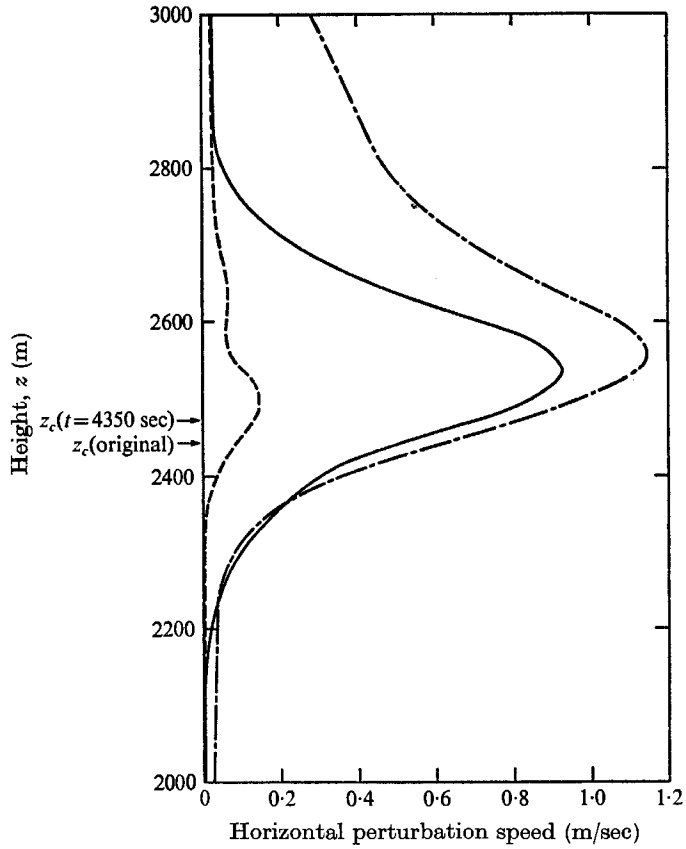

FIGURE 6. The magnitude of the Fourier components of the horizontal component of the perturbation velocity at t = 4350 sec. S_s = 1·125 m/sec; Ri = 0·53; — · —, fundamental; ——, constant; - - -, second harmonic.

It is clear from the contour plots in figure 2 that a situation very close to the steady state has been reached in the latter stages of this case. The attainment of near steady state is also borne out by various other figures. For example, the maximum values of the absolute values of the fundamental of u and ρ reach their peaks of 1·75 m/sec and 0·00242 kg/m^3 respectively at 2190 sec and by 3630 sec these values have dropped back to 1·17 m/sec and 0·00150 kg/m^3 and they oscillate about these values thereafter. The minimum Richardson number present at any time has its lowest value, 0·321, at 2910 sec and by 3630 sec it has returned to 0·350 where it hovers thereafter. The change in the wind

continues to grow, of course, but its growth is slow, the absorption of new momentum being offset to some extent by the slow diffusion of momentum outward from that height where the change is greatest. It appears that the increase in the change in the wind and its diffusion, and the amount of incident energy and momentum absorbed by the shear layer are balanced in such a way as to maintain the minimum Ri at 0·35.

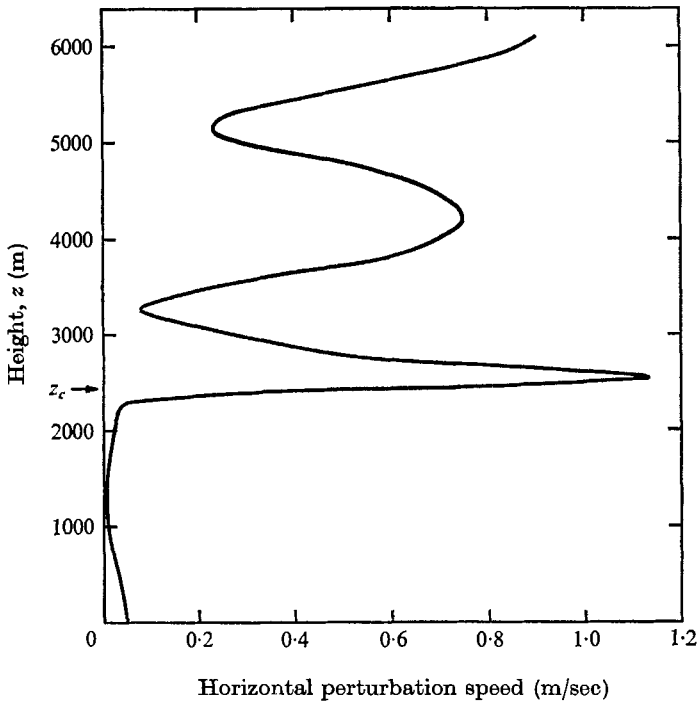

FIGURE 7. The magnitude of the fundamental component of the horizontal component of the perturbation velocity. t = 4350 sec, S_s = 1·125 m/sec, Ri = 0·53.

It is impossible to separate accurately the upgoing and downgoing wave components in a finite-difference model such as the one reported here but from the values of the peaks and nodes of the components of the perturbation motion above and below the shear layer one can estimate the portions of the incident wave energy which are being reflected and transmitted. Because the kinetic energy of the vertical motions is easily derived from the kinetic energy of the horizontal motions only the portions of the horizontal kinetic energy which are reflected and transmitted have been calculated. In figure 7, for example, the maximum at 4200 m is the sum of the contributions of the upgoing and the downgoing wave, $u_{\max} = u_{\text{down}} + u_{\text{up}}$, while the minimum at 3300 m represents their difference, $u_{\min} = u_{\text{down}} - u_{\text{up}}$, and the reflectance would be $(u_{\text{up}}/u_{\text{down}})^2$. (Over-reflectance in which u_{up} is greater than u_{down} may be distinguished by the sign of the Reynolds stress.) For this reference case at t = 4350 sec about 40 % of the incident horizontal kinetic energy was being reflected and about 0·2 % was being transmitted. Because the second and higher harmonics are evanescent

outside the shear layer, only the fundamental need be considered in these calculations. It is clear from figure 1 (*a*) that these reflectance and transmittance values depend somewhat on the spacing but no great accuracy is claimed for these figures in any event.

For comparison, in the steady-state case, where there is no shear layer and the wind speed changes abruptly from 20 m/sec to zero, the linear solutions, ignoring the presence of a critical level, give a reflectance of 65% and a transmittance of 0·01 %. For further comparison, this case was run with the non-linear terms removed from the model and the reflectance was about 20 % and the transmittance about 0·4 %. (These numbers refer to the kinetic energy of the horizontal component of the x-dependent motion.) The non-linear coupling between the incident wave and the wind and the resulting change in the wind somehow approximately doubles the size of the reflected wave but no details as to the basic mechanism by which this is accomplished are available. The other major difference between the non-linear and the linear model, in addition to the lack of any coupling to the mean flow or higher harmonics in the linear model, was that the maximum of the fundamental of u was about 60 m lower in the linear model than in the non-linear model.

For this reference case then, it appears that slightly more than half of the horizontal kinetic energy of the incident wave is being absorbed in the shear layer. It is difficult to ascertain how much of this energy goes into the mean flow and how much goes into shorter wavelengths and eventual turbulent dissipation, but it appears from this model that the bulk of the energy goes into the mean motion. The wind speeds outside the shear layer are such that perturbations whose horizontal wavenumbers are integer multiples of the source wavenumber are evanescent outside the shear layer, so that any energy in these modes is trapped within the shear layer.

In addition to having $S_s = 1{\cdot}125$ m/sec, the case in which the Richardson number was originally 0·53 was also run with source strengths of 0·281, 2·250 and 5·625 m/sec. With $S_s = 2{\cdot}250$ m/sec the portions of the incident wave being reflected and transmitted at $t = 4350$ sec and the minimum Ri were almost identical to those for $S_s = 1{\cdot}125$ m/sec. The maximum values of the absolute values of the fundamental component of u and of the change in the wind were, however, about twice as large and were located at about 2600 m instead of 2550 m for the smaller source. The possibility that the reflectivity and transmittivity depends only on the minimum value of Ri was ruled out by the results with $S_s = 0{\cdot}281$. Here the system reached a nearly steady state about 3000 sec but the minimum Ri never fell below 0·50, yet the reflectivity was only slightly lower, about 30 %. With such a small incident wave there was very little change in the wind.

The results are difficult to interpret for the largest source, $S_s = 5{\cdot}635$ m/sec. The incident wave was so large that non-linear interactions near the source and far from the shear layer created a jet there, driving the total wind speed below the horizontal phase speed of the source and creating another critical level. The wind change was also large just above the critical level but the maximum of the wind change was very close to the top of the shear layer and therefore no region

of high shear and low Ri appeared. As this case progressed the Reynolds stress became negative over much of the height range above the critical level, which had been as high as 2760 m and began to move downward as the change in the wind decreased. Because of the large non-linear interactions which occurred outside the shear zone such large sources were avoided thereafter.

Before discussing the effect of varying the Richardson number one additional case must be mentioned. To ascertain whether the discontinuous shear of the piecewise linear wind profile had a major effect on the events near the critical

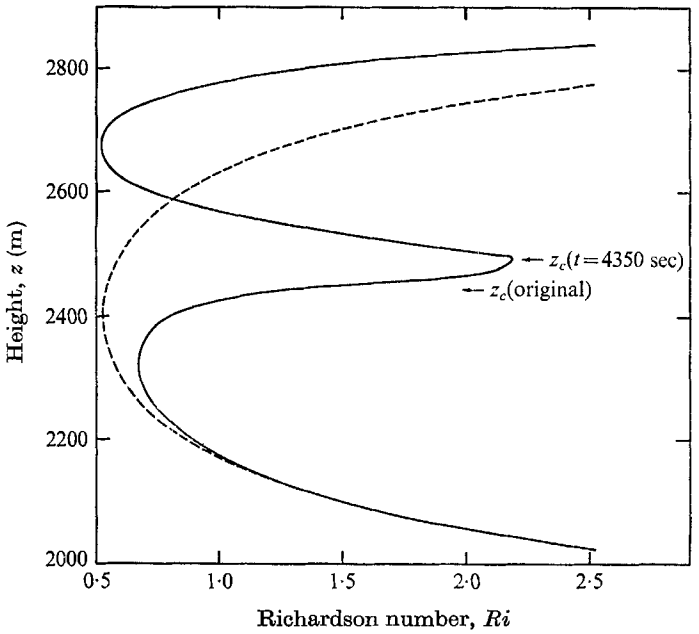

FIGURE 8. Richardson number for the case where the wind was originally a hyperbolic tangent function of the height. S_s = 1.125 m/sec; – – –, original; ——, t = 4350 sec.

level the term involving the second derivative of the wind was added to the equations and the Ri = 0·53, S_s = 1·125 m/sec case was run with a hyperbolic tangent wind profile. The maximum shear and minimum Ri were the same as for the linear wind profile, but in this case they pertain only to the midpoint of the shear layer, z = 2400 m. The Richardson number as a function of height is plotted in figure 8. For this wind profile the portion of the incident wave which was transmitted was about 0·6 % and the portion reflected was about 30 %. The maximum change in the wind was about twice as great as with the linear wind profile and was centred about 50 m higher. The minimum Ri remained around 0·52 after 2900 sec but maximum of the absolute value of the fundamental component of u did not stop increasing as it had done in the other cases. The details of the critical level interaction, then, depend on the wind profile but the basic nature of the interaction does not.

The case in which the Richardson number was 2·12 was run for source strengths of 1·125 and 0·281 m/sec. The development was much the same as in the Ri = 0·53

cases except that the pace of the interaction was much slower, that is, at $t = 4350$ sec the steady state had not been reached for either source. The minimum Richardson number was still decreasing at 4350 sec and was 0·67 for the larger source and 1·88 for the smaller. At this time, for both sources, about 10^{-4} of the incident energy was being transmitted through the shear layer. The incident wave energy reflected was about 4 % with the larger source and 9 % for the smaller source.

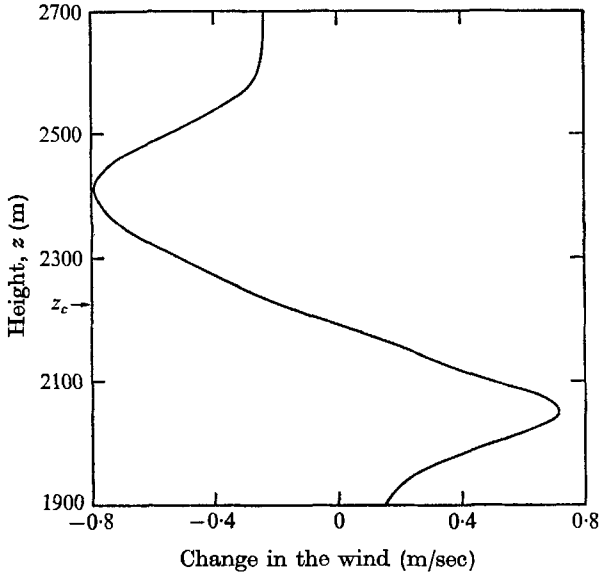

FIGURE 9. Change in the wind. $S_s = 1{\cdot}125$ m/sec, $Ri = 0{\cdot}13$, $t = 3270$ sec.

For the case of a dynamically unstable shear, $Ri = 0{\cdot}133$, source strengths of 1·125 and 0·281 m/sec were used. For the larger source the results blew up at 3540 sec but with the smaller source the program ran to termination at 4500 sec as usual. The change in the wind is shown in figure 9. The positive wind change below the critical level was not present when the Richardson number was greater than 0·25. Furthermore, there were large abrupt fluctuations in the Reynolds stress. For the large source, for example, the Reynolds stress which had been large and negative below 4500 m at 2550 sec was large and positive by 2910 sec everywhere except in the shear layer, where it remained negative. For both sources about 6 % of the incident energy was being transmitted just before the program terminated, but with the larger source about 35 % of the incident energy was being reflected at 3270 sec while for the smaller source about 130 % of the incident energy was being reflected at 4350 sec. In the case of the smaller source the Reynolds stress is negative from the ground to 5000 m, so that the larger component is the upgoing wave rather than the usual downgoing wave and over-reflexion is taking place.

5. Conclusions

The results of this model were different from those of the linear predictions in that a large portion of the energy was reflected from the critical level. Also the portion of the wave transmitted through the critical level was considerably below that predicted by Booker & Bretherton (1967) for low Richardson numbers

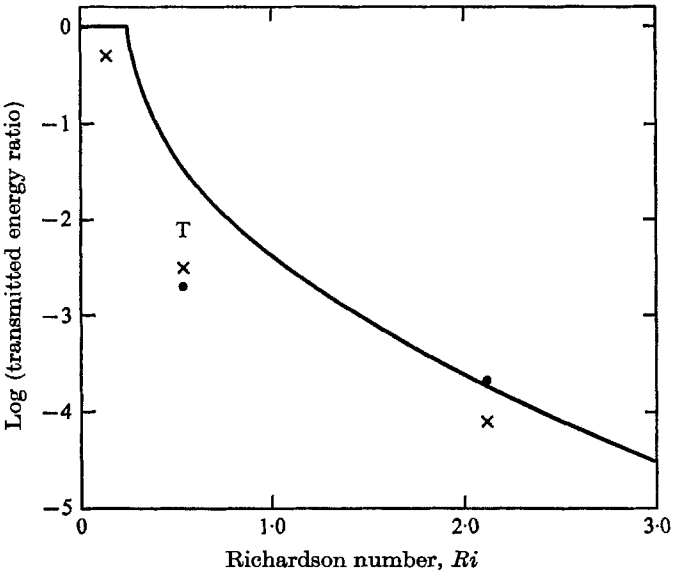

FIGURE 10. The ratio of the kinetic energy of the horizontal wave motion transmitted through the shear layer of that incident upon the shear layer, as a function of Richardson number. ●, S_s = 1·125; ×, S_s = 0·281; T, Tanh wind, S_s = 1.125.

as shown in figure 10. In the case where originally $Ri = 2{\cdot}12$ the portion of the incident wave's energy transmitted is fairly well estimated by Booker & Bretherton (1967). The conclusion from their work and the present study is that for large Richardson numbers a negligible amount of energy is transmitted through the critical level and most of the incident momentum and energy is absorbed near the critical level.

It seems safe to conclude that a shear layer containing a critical level with a Richardson number less than about 1·0 is sufficiently reflective to act as a leaky boundary and cause trapping. No explicit predictions of this on the basis of the linear theory are known, but in general linear wave theory it is well known that any substantial change in the impedance of the propagation medium in a distance short compared to the appropriate wavelength will cause reflexions. If an internal gravity wave is to be propagating (as opposed to evanescent) in zero-shear layers above and below the shear layer, then a Richardson number less than unity implies a shear so large that the maximum extent of the shear layer will be some fraction of the vertical wavelength (calculated for one of the zero-shear layers) and thus this reflexion could have been foreseen from the linear theory. The contention of Jones (1968) that over-reflexion would occur when the Richardson number was

less than 0·25 has been borne out (as shown by the sign of the Reynolds stress). No steady state with over-reflexion was ever reached in the present model but with the basic system being dynamically unstable this is not surprising.

It would be helpful if the amount of incident energy reflected depended in some simple way on the wave magnitude, the overall Ri or the local Ri, but such a relationship has not been observed. About all that can be said is that the reflectivity is about 35 % in the case where Ri was 0·53 originally, about 7 % in the case where Ri was 2·12 originally, and that reflectivity probably becomes negligible for Richardson numbers greater than 5.

As mentioned above, in the case where the large ($S_s = 5{\cdot}635$ m/sec) source was used non-linear interactions near the source generated a jet, and eventually a critical level, in a region which was initially free of shear. From this it may be concluded that for regions of zero shear when the horizontal component of the perturbation velocity approaches or exceeds 10 % of the horizontal component of the phase velocity, the non-linear effects will cause significant changes in the average motion of the atmosphere and, if these forces act for a sufficient length of time, a jet will eventually develop, perhaps followed by the appearance of a critical level if the magnitude of the jet increases sufficiently. The development of a critical level depends on the rate at which the wave puts momentum into the jet compared to the rate at which the viscosity causes the jet to become more diffuse. For $\mu = 2$ kg/msec it appears that when the ratio $|u|/v_{px}$ is about 15 % the jet will continue to grow until a critical level is present, but if this ratio is about 10 % the maximum speed of this jet falls far short of that necessary to give a critical level. There is then, a maximum amplitude for the unhindered propagation of internal gravity waves and a wave exceeding this value will create its own critical level and be largely absorbed into the mean flow there.

There are two aspects of this study that may need further clarification. First, this study has been strictly two-dimensional whereas gravity waves in the real atmosphere are of a scale that is not entirely three-dimensional and yet cannot be represented in two dimensions to one's complete satisfaction. Because of the basic difference of turbulence in two and three dimensions and the tendency for motions to move to larger scales in two dimensions and to move to smaller scales in three dimensions (Onsager 1949; Fjörtoft 1953), it is possible that the division of the absorbed energy between the mean flow and smaller scales of motion and eventual turbulence shown by this model may not correspond accurately to the real atmosphere. Until sufficiently detailed experiments are conducted or three-dimensional computer models become less expensive, this matter will have to remain open.

Further, some authorities may claim that the top and bottom boundaries have a significant effect on the events around the critical level in this model. The author does not believe this to be true. It is certainly true that the wave which passes through the shear layer is reflected by the lower boundary. The wave below the shear layer is observed to be very nearly a perfect standing wave. However, the magnitude of the wave entering the shear layer from below is always so much smaller than the wave entering from above that its effects are negligible. Further, no effects of a wave entering the shear layer from below have

been observed. As for the upper boundary, the nature of the mirroring is such that until the incident downgoing wave has been reflected and made its way back to the source there is no possibility of the upper boundary influencing events. It is possible that in the latter stages of the cases in which the reflectivity was highest the top boundary condition has the effect of increasing the source strength by reflecting the upgoing wave back down again. If this is true it has taken place in such a way that the additional downgoing wave motion is in phase with that from the source which, although possible, seems rather unlikely.

This research was initiated at the Massachusetts Institute of Technology (a portion of it forms part of the authors doctoral thesis) and was completed at the National Center for Atmospheric Research. The work at M.I.T. was supported by the U.S. Army Research Office, project number 2MO14501B52B, contract number DA-31-124-ARO-D-431. The National Center for Atmospheric Research is sponsored by the National Science Foundation. I am grateful to T. R. Madden and W. L. Jones for many helpful discussions.

REFERENCES

Booker, J. R. & Bretherton, F. P. 1967 *J. Fluid Mech.* **27**, 513.

Bretherton, F. P. 1966 *Q. J. Roy. Met. Soc.* **92**, 394.

Fjörtoft, R. 1953 *Tellus*, **5**, 225.

Foldvik, A. & Wurtele, M. G. 1967 *Geophys. J. Roy. Astron. Soc.* **13**, 167.

Hazel, P. 1967 *J. Fluid Mech.* **30**, 775.

Jones, W. L. 1967 *J. Fluid Mech.* **30**, 430.

Jones, W. L. 1968 *J. Fluid Mech.* **34**, 609.

Lilly, D. K. 1965 *Mon. Weather Rev.* **93**, 11.

Madden, T. R. & Claerbout, J. F. 1968 Jet stream associated gravity waves. In *Acoustic Gravity Waves in the Atmosphere.* Proc. of ESSA/ARPA Symposium at Boulder, Colorado (ed. T. M. Georges), pp. 121–134. Washington, D.C.: U.S. Government Printing Office.

Onsager, L. 1949 *Nuovo Cimento Suppl.* **6**, 279.

Richtmyer, R. D. 1957 *Difference Methods for Initial-Value Problems.* Interscience.